Structural Studies of the Contractile Tail Sheath Protein of Bacteriophage T4. 1. Conformational Change of the Tail Sheath upon Contraction As Probed by Differential Chemical Modification†

Shigeki Takeda,‡ Fumio Arisaka,‡,* Shin-ichi Ishii,‡ and Yoshimasa Kyogoku§

Department of Biochemistry, Faculty of Pharmaceutical Sciences, Hokkaido University, Sapporo, Japan 060, and Institute of Protein Research, Osaka University, Suita, Osaka, Japan 565

Received August 10, 1989; Revised Manuscript Received November 28, 1989

ABSTRACT: Differential chemical modifications of tyrosine residues of the tail sheath protein, gp18, were performed to elucidate the structural change of the tail sheath upon contraction. Tyrosine residues of monomeric gp18, extended tail sheath, and contracted tail sheath were nitrated by tetranitromethane, and the modified tyrosine residues in each state of the sheath protein were identified by peptide mapping and amino acid sequence analyses of the isolated peptides. Of 31 tyrosine residues in gp18 monomer or in the extended sheath, 12 or 13 residues (Tyr63 and/or -73, -225, -254, -270, -304, -455, -460, -493, -532, -535, -569, and -590) were modified. When photo-CIDNP difference spectra were measured with monomeric gp18, two peaks, which are due to highly exposed tyrosine residues on the molecular surface of gp18, were observed. These two peaks disappeared when the monomeric gp18 was nitrated. With contracted sheath, however, only eight tyrosine residues (Tyr225, -254, -270, -455, -460, -493, -532, and -535) were nitrated on the contracted sheath. Chemical modification of cysteine residues by sulfhydryl group specific reagent ABD-F [(4-aminosulfonyl)-7-fluoro-2,1,3-benzoxadiazole] revealed that, among five cysteine residues, Cys377, Cys477, and Cys607 have a sulfhydryl group. Cys402 and Cys406 were modified only under reducing conditions, which strongly suggested the presence of a disulfide bond between these two residues.

Striking structural changes are observed in the morphogenesis and infection process of bacteriophage T4. One example is the expansion of the prohead during the phage head morphogenesis. After specific cleavage of most of the head proteins including the major capsid protein (Black & Showe, 1983), gp23 (gp, gene product), by the action of T4 prohead proteinase (T4PPase), gp21, which is itself cleaved by the proteinase, the head expands approximately 15% (Kellenberger, 1968), which increases the volume by 50%. The significance of the process is not totally understood, but it is an important step toward maturation of the head. The prohead which originally enclosed the "scaffolding proteins" changes its state to that which is now able to accommodate the genomic DNA of the phage. The resultant expanded head is much more resistant to dissociation than prohead and is known to be antigenically distinct from prohead (Favre et al., 1965; Yanagida, 1972).

On the other hand, the most striking structural change upon infection is the contraction of the tail sheath which is triggered by the expansion of the baseplate. Upon adsorption to the host bacterium, the baseplate changes its shape from a hexagon to a star (Simon & Anderson, 1967; Crowther et al., 1977), and this structural transformation induces contraction of the sheath. The extended tail sheath, 95 nm long and 20 nm in diameter, becomes 38 nm long and 25 nm in diameter upon contraction (Brenner et al., 1959; Kellenberger & Boy de la Tour, 1964; King & Mykolajewycz, 1973). The resultant contracted sheath is known to be very stable, being resistant to 6 M Gdn·HCl[1] at room temperature (To et al., 1969). The tail sheath consists of 144 protomers of the sheath protein, gp18, arranged in 24 annuli (Moody, 1973). Recently, we determined the primary structure of gp18 as the first step toward elucidation of the mechanism of contraction (Arisaka et al., 1988). In this paper, we describe the results of differential chemical modification of tyrosine residues on the molecular surface of gp18 before and after contraction. The results of examination on the reactivities of five cysteine residues are also included.

Materials and Methods

Enzymes and Reagents. DNase I and trypsin (bovine pancreas) were purchased from Sigma Chemical Co. Lysyl endopeptidase, a lysine-specific serine protease from *Acromobacter lyticus* M467-1, was purchased from Wako Junyaku Co. Trypsin purchased from Sigma was further purified by affinity chromatography (Kumazaki et al., 1986) and treated with L-1-(tosylamino)-2-phenylethyl chloromethyl ketone (TPCK). ABD-F (7-fluoro-4-sulfamoyl-2,1,3-benzoxadiazole) and SBD-F (ammonium 7-fluoro-2,1,3-benzoxadiazole-4-sulfonate) were a kind gift from Dr. K. Imai at the University of Tokyo in the early phase of the study and later purchased from DOJINDO Laboratories Co. All other reagents were of analytical grade from Nakarai Chemicals or Wako Jun-yaku. Nutrient broth, bactotryptone, yeast extract, bactoagar, and casamino acids were purchased from DIFCO Laboratories.

Media and Buffer. M9A medium was used to grow *Escherichia coli*. It contained, per liter of water, 6 g of Na_2H-

† This work was supported by Grant-in-Aids for Scientific Research from the Ministry of Education, Science, and Culture of Japan.

* Address correspondence to this author at his present address: Department of Life Science, Tokyo Institute of Technology, 4259 Nagatsuta, Midori-ku, Yokohama, Japan 227.

‡ Hokkaido University.

§ Osaka University.

[1] Abbreviations: TCA, trichloroacetic acid; HPLC, high-performance liquid chromatography; SDS, sodium dodecyl sulfate; TNM, tetranitromethane; ABD-F, 7-fluoro-4-sulfamoyl-2,1,3-benzoxadiazole; SBD-F, ammonium 7-fluoro-2,1,3-benzoxadiazole-4-sulfonate; Gdn·HCl, guanidine hydrochloride; CIDNP, chemically induced dynamic nuclear polarization.

0006-2960/90/0429-5050$02.50/0

PO_4, 3 g of KH_2PO_4, 0.2 g of $MgSO_4 \cdot 7H_2O$, 0.5 g of NaCl, 1 g of NH_4Cl, 4 g of glucose, and 10 g of casamino acids. Phages were stored in B^+ buffer which contained, per liter of water, 7 g of Na_2HPO_4, 4 g of NaCl, and 3 g of KH_2PO_4, supplemented with 1 mM $MgSO_4$ for use.

Phage and Bacterial Strains. T4D wild-type phage and T4D.23amH11 are from our collection. *E. coli* BE was used as a nonpermissive host for amber mutant phages, and *E. coli* CR63 was the permissive host.

Preparation of Tails and Gp18. Tails and gp18 were prepared according to the method of Tschopp et al. (1979). Monomeric gp18 thus prepared was used within a week. Tails, which are the immediate source of monomeric gp18, could be stored for several months as a solution with 0.02% sodium azide at 4 °C without loss of activity as judged by the reassociation ability of isolated gp18.

Preparation of Contracted Sheaths. Contracted sheaths were isolated according to the method of Sarker et al. (1964). T4D phage particles, which was the source of contracted sheaths, were purified by CsCl step gradient centrifugation (Dickson, 1974).

Nitration of Tyrosine Residues of Gp18. Tails were used as the materials for nitration of gp18 either in the monomeric state or in the extended sheath. When monomeric gp18 was to be nitrated, tails were dialyzed against 0.1 M borate buffer, pH 9.0, at 4 °C overnight. Under these conditions, sheaths were completely dissociated into monomeric gp18 as examined by electron microscopy (data not shown). At pH 9.0, the backbone structure of gp18 does not alter for at least a week as examined by far-ultraviolet circular dichroism spectra (data not shown; also, Arisaka and Yutani, unpublished results). When extended sheaths were to be nitrated, 5 mM $MgSO_4$ was added to the tail solution of 0.1 M sodium–potassium phosphate, pH 7.2, and the tail solution was then dialyzed against 0.1 M borate buffer–5 mM $MgSO_4$, pH 9.0, at 4 °C overnight. Tails thus prepared were examined by electron microscope, and it was confirmed that they were sheathed (data not shown). Thirty times molar excess of tetranitromethane (TNM) dissolved in ethanol over gp18 was added to thus prepared monomeric gp18 or tails with extended sheath; less than $^1/_{100}$ volume of TNM–ethanol solution was added to the solution so that ethanol was sufficiently diluted. The reaction mixture was incubated at 20 °C for the desired time, and the reaction was stopped by adding $^1/_{500}$ volume of 2-mercaptoethanol. The solution was then dialyzed against 1 mM phosphate buffer, pH 7.2, overnight. When monomeric gp18 was modified, tube–baseplates were removed by differential ultracentrifugation after dialysis; the dialyzate was centrifuged at 140000*g* for 2 h, and the supernatant was recovered. When extended sheaths were nitrated, the reaction mixture after dialysis was mixed with an equal volume of 2 M urea in 1 mM phosphate buffer, incubated at 4 °C for 30 min to dissociate sheaths, and centrifuged to recover supernatant.

Contracted sheaths were nitrated in the same way as above except that the sample solution in 0.1 M phosphate buffer after nitration was further dialyzed against distilled water and lyophilized. The lyophilized sheaths were then dissolved in 6 M Gdn·HCl–10 mM Tris·HCl, pH 8.0, and denatured at 100 °C for 10 min. Gdn·HCl was removed after carboxymethylation (see below) by dialysis against 1 mM phosphate buffer, pH 7.2.

Carboxymethylation of Thiol Groups of Gp18. Gp18 and nitrated gp18 were S-carboxymethylated under reducing conditions according to the method of Ruegg and Rudinger (1977). Approximately 3 mg of gp18 was dialyzed against 1 mM phosphate buffer, pH 7.2, dried in a centrifugal concentrater, and dissolved in 0.7 mL of 6 M Gdn·HCl–0.1 M Tris·HCl, pH 8.2. To the solution was added 0.3 mL of *n*-propanol. After the pH was verified to be between 8.0 and 8.3, 30 μL or 2% (v/v) tri-*n*-butylphosphine in *n*-propanol was added, and the solution was incubated for 2 h. Three microliters of 1 M sodium iodoacetate–1 M sodium hydroxide was added to the solution, shielded from light, and incubated at room temperature. Three microliters of 2-mercaptoethanol was added at 40 and 60 min after addition of iodoacetate to exhaust the excess reagent. The reaction mixture was then extensively dialyzed against 10 mM Tris-HCl buffer, pH 8.2. During dialysis, the solution was shielded from light.

Lysyl Endopeptidase Digestion of Gp18. Gp18, nitrated and S-carboxymethylated as described above, was extensively digested with lysyl endopeptidase in the weight ratio of 1/500 at 37 °C for 12 h. Unmodified gp18 in 1 mM phosphate buffer, pH 7.2, was denatured at 90 °C for 10 min prior to digestion. Ten percent formic acid was added to the solution to pH 3, and the solution was subjected to HPLC.

Arylation of Thiol Groups of Gp18 with ABD-F. Gp18 in the monomeric state and that in the extended sheath were chemically modified by ABD-F according to the method of Toyo'oka and Imai (1984). When monomeric gp18 was modified, tails were dialyzed against 1 mM borate buffer, pH 8.0 at 4 °C, overnight. If gp18 in the extended sheath was to be modified, tails were dialyzed against 0.1 M borate buffer, pH 8.0. In either case, the state of gp18, extended sheath or monomeric, was checked by electron microscopy. When denatured gp18 was to be modified, the monomeric gp18 that had been prepared as above was freed from coexisting tube–baseplates by centrifugation at 140000*g* for 2 h. Solid Gdn-HCl was added to the supernatant to a final concentration of 6 M. If the sample was to be reduced, $^1/_{50}$ volume of 2% tri-*n*-butylphosphine in *n*-propanol was further added, and the mixture was incubated for 2 h. To the control solution, the same volume of *n*-propanol was added.

To the solution of gp18 thus prepared was added ABD-F (10 mM in water) to a final concentration of 0.5 mM. After incubation at 40 °C for 30 min, the mixture was dialyzed against 10 mM Tris·HCl, pH 8.3, at 4 °C overnight.

Trypsin Digestion of Gp18. Trypsin was added to gp18 modified with ABD-F as described above in the weight ratio of 1/100. After incubation at 37 °C for 2 h, the TPCK-treated trypsin was added again in the weight ratio of 1/100, and incubation at 37 °C was continued for further 12 h. The reaction was stopped by heating in boiling water for 3 min, and TCA was added after cooling, to a final concentration of 5%. After removal of precipitates by centrifugation at 2300*g* for 15 min, TCA was removed by ether extraction and water was removed by evaporation. The gp18 digest was dissolved in water at approximately 4 mg/mL, and insoluble materials were removed by using a 0.45-μm Millipore filter before application to HPLC.

HPLC of Gp18 Digests. Peptides were separated on a reversed-phase HPLC system (Waters 600) equipped with a gradient former, a degasser (Erma ERC-3510), UV and fluorescence monitors (Waters 490 and Shimadzu RF530, respectively), and a column of Nucleosil $5C_{18}$ (0.4 × 25 cm). Two hundred microliters of a sample solution was applied to the system, and the effluent was manually fractionated. Elution conditions will be described in the figure legends.

Amino Acid Analysis. Amino acid compositions of peptides without nitrated tyrosine were determined by the phenyl-

thiocarbamylation (PTC) method after hydrolysis with 6 M HCl–1% phenol in vapor phase at 110 °C for 24 h on the Pico-tag work station (Waters Co.) according to the manufacturer's specifications. Twenty microliters of redrying solution (volume ratio of ethanol:water:triethylamine = 2:2:1) was added to the hydrolysate, and it was dried again in vacuum. After addition of 10 μL of the reagent solution (volume ratio of ethanol:water:triethylamine:phenyl isothiocyanate = 7:1:1:1), the mixture was incubated for 20 min at room temperature, and the reaction was stopped by drying in vacuum (>60 min). The PTC amino acids thus obtained were analyzed by HPLC. Amino acid compositions of the whole protein and peptides with nitrated tyrosines were determined on an amino acid analyzer (Hitachi 835) equipped with a ninhydrin monitor after hydrolysis in 20 μL of 6 M HCl–2% 2-mercaptoethanol at 110 °C for 24 h.

Sequence Determination of Peptides. Amino acid sequences of peptides were determined on a pulsed liquid protein sequencer, Applied Biosystems 477A. Usually, 0.5–1 nmol of sample was applied and analyzed. PTH amino acids were analyzed and identified by HPLC.

NMR Spectra Measurements. ^{1}H photo-CIDNP (photochemically *i*nduced *d*ynamic *n*uclear *p*olarization) spectra of monomeric gp18 with and without nitration were taken at 500 MHz on a JEOL GX-500S NMR spectrometer by using an especially designed probe with a 3-mm quartz rod to introduce a laser light. Ten milliliters of tail solution (A_{280} = 1.2) in 0.1 M phosphate buffer, pH 7.2, was subjected to ultracentrifugation (140000*g*, 1 h), and the pellet was dissolved in 0.5 mL D_2O and dialyzed three times against 10 mL of 1 mM phosphate buffer in D_2O, pD 7.0. Under these conditions, gp18 was completely dissociated from tube–baseplates as checked by electron microscopy. Coexisting tube–baseplates whose molecule weight amounts to approximately 10^8 were considered to be nonvisible by NMR.

Results

Chemical modification was used to study the higher order structure and its change of the tail sheath protein of phage T4. Tyrosine residues were chosen as the target residue because they are distributed reasonably evenly in the primary structure and because, due to the medium value of hydrophobicity, the probability of finding tyrosine side chains inside and outside a globular protein will be comparable. TNM was used as a reagent, which generally nitrates only exposed tyrosine residues of which the hydroxyl group is free. Also, nitration of tyrosine residues was expected to depend on the association state of the gp18 molecule, namely, the monomeric form, the extended state, and the contracted state of the tail sheath.

Nitration of Tyr Residues in Monomeric Gp18. To identify tyrosine residues that are exposed to the solvent, gp18 was nitrated with TNM. Gp18 contains totally 31 tyrosine residues which are distributed in 16 lysyl endopeptidase fragments (Table I). First, the time course of the nitration was followed under the conditions described under Materials and Methods. The extent of reaction reached a plateau by 90 min, when approximately 12 tyrosine residues were nitrated as determined by amino acid analysis (Figure 1). Circular dichroism spectra of the nitrated gp18 in the far-UV region demonstrated that the secondary structure of gp18 did not change during nitration for as long as 120 min (data not shown).

After nitration at 20 °C for 90 min, gp18 was thoroughly digested with lysyl endopeptidase and anlyzed by HPLC. The elution profile was compared with that of digests of nonmodified gp18 (Figure 2). In the chromatogram, eluates were monitored with absorption at 280 nm so that only those peptides that contain tyrosine or tryptophan residues were detectable. As shown in Figure 2b, peaks K-4, K-18, K-19, K-24, K-25, K-26, and K-29 have reduced their heights after nitration, and some new peaks appeared as indicated by K-18(1), K-24(1), K-24(2), and so on. In Figure 3, the time course of nitration of these peptides except for K-18 are plotted as monitored by the decrease in peak heights; quantitative measurements of the change in the peak height of K-18 were hampered by occasional overlap with peak K-5. Newly appeared peaks shown in Figure 2b were then fractionated and rechromatographed, and the amino acid sequence analyses were performed. These peaks were thus identified to be K-18, K-19, K-24, K-25, K-26, and K-29, of which tyrosine residues 254, 270, 455, 460, 493, 532, 535, and 590 were nitrated.

Table I: Summary of Tyrosine Nitration

peptide	tyrosine	nitration[a] *b*	*c*	*d*	comment
K-4	Tyr63	+	++	–	
	Tyr73	+	++	–	
K-5	Tyr100	–	–	–	*h*
	Tyr109	–	–	–	*h*
K-7	Tyr119	–	–	–	*h*
K-13	Tyr159	–	–	–	*h*
K-15	Tyr216	–	–	–	*h*
	Tyr225	+	+	+	*e*, *h*
K-17	Tyr243	–	–	–	*h*
K-18	Tyr254	+	++	++	*f*, *h*
K-19	Tyr270	++	++	++	*h*
	Tyr278	–	–	–	*h*
K-21	Tyr304	+	+	–	*h*
	Tyr309	–	–	–	*h*
K-22	Tyr321	*	*	*	*g*
K-23	Tyr435	–	–	–	
	Tyr446	–	–	–	
	Tyr453	–	–	–	
K-24	Tyr455	+++	+	++	
	Tyr457	–	–	–	
K-25	Tyr460	+++	++	+	
	Tyr493	+++	++	+	
K-26	Tyr517	–	–	–	
	Tyr532	+++	++	+	
	Tyr535	+++	++	+	
K-29	Tyr569	+++	+++	–	
	Tyr590	+++	+++	–	
K-30	Tyr601	*	*	*	*g*
	Tyr603	*	*	*	*g*
	Tyr627	*	*	*	*g*
	Tyr636	*	*	*	*g*

[a] Degrees of nitration are expressed as a percentage of decrease in peak heights of unmodified peptide; (+++) 100–75%; (++) 75–50%; (+) 50–20%; (–) 20–0%. [b] Monomeric gp18. [c] Extended sheath. [d] Contracted sheath. [e] Peptide K-15 tends to superimpose on K-3. [f] Peptide K-18 tends to superimpose on K-5. [g] Not examined in the present study. [h] Trypsin-resistant region.

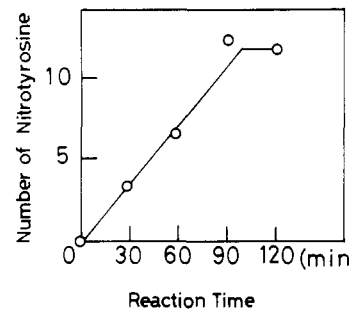

FIGURE 1: Time course of nitration of tyrosine residues. Monomeric gp18 was nitrated by tetranitromethane, and the nitrated tyrosine residues per gp18 protomer were quantitated by amino acid analysis. Approximately 12 tyrosine residues/gp18 were modified in 90 min.

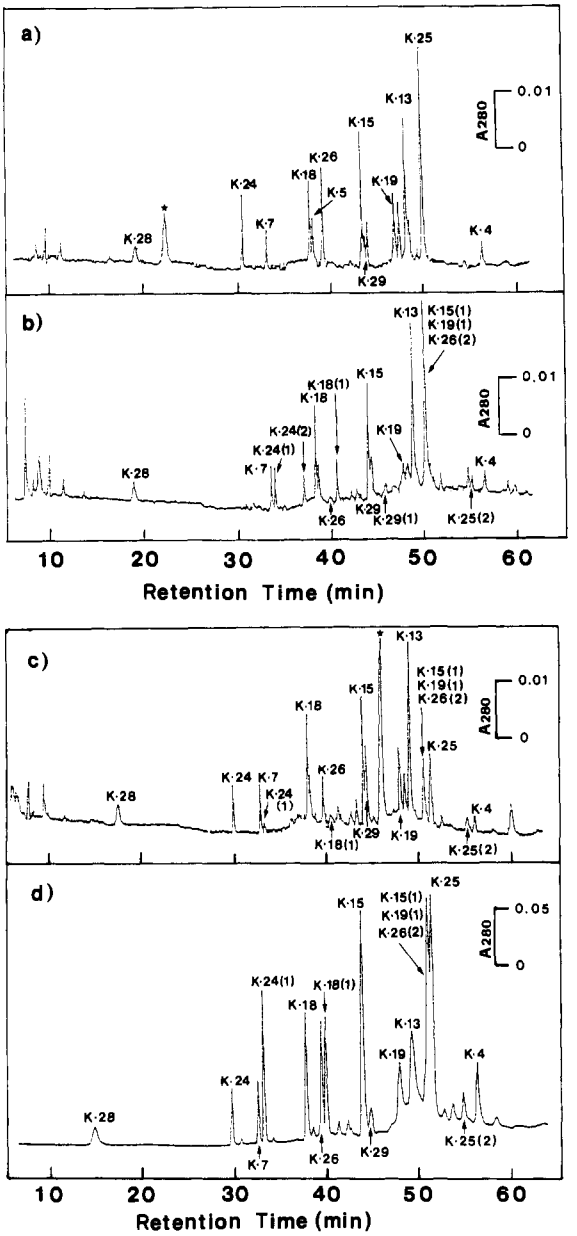

FIGURE 2: HPLC elution profiles of lysyl endopeptidase digests of gp18 (a) before and (b–d) after nitration [for (b) and (c), nitration for 90 min; for (d), nitration for 120]. See Arisaka et al. (1988) for peptide serial number. A number (1 or 2) in parentheses preceded by the peptide number denotes the number of nitrated tyrosine residues. Note that the total amount of the sample was not exactly the same for all the experiments (a–d). The peak height of K-7 or K-13 can be taken as an internal standard, because they were not nitrated at all. Solvent conditions are as follows: 0.1% trifluoroacetic acid, acetonitrile 8% → 32% (15 min) → 60% (45 min); flow rate 1 mL/min. Nucleosil $5C_{18}$ column was used. (★) Peak of reagent origin.

Since we could not identify nitrated peptide K-4, it is not certain if both Tyr63 and Tyr73 were nitrated or only one of them. As for peptide K-29, nitration is considered to have occurred at both Tyr535 and Tyr590, although the peptide with the two nitrated residues was not identified. This is because peptide K-29 in which only Tyr590 had been nitrated also decreased during the nitration reaction. The results are summarized in Figure 4 and Table I. Apparently, tyrosines in the C-terminal half of gp18 molecule are nitrated better than those in the N-terminal half.

With this method, nitration of Tyr321 in peptide K-22 was not observable because the peptide has not been identified on HPLC (Table I). The peptide is expected to contain 74 amino acid residues and is rather hydrophobic (Arisaka et al., 1988).

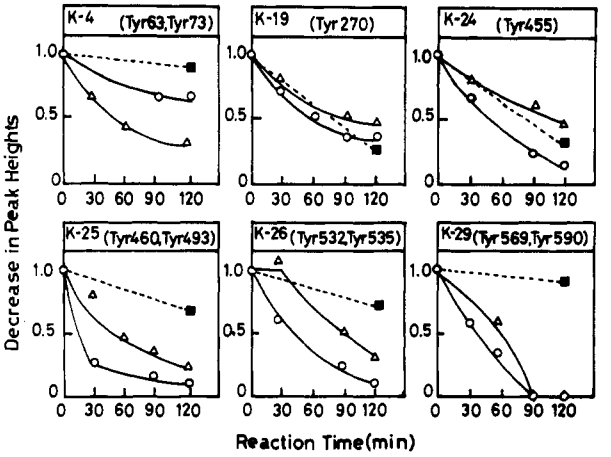

FIGURE 3: Time course of nitration on tyrosine residues of gp18 in various forms as monitored by decrease in HPLC peak heights due to peptide fragments. Peak heights of tyrosine-containing peptides as shown in Figure 2 are measured and plotted with respect to time. As internal standards, peak heights of peptides such as K-7, which are not nitrated, were measured. (○) Monomeric gp18; (△) extended sheath; (■) contracted sheath.

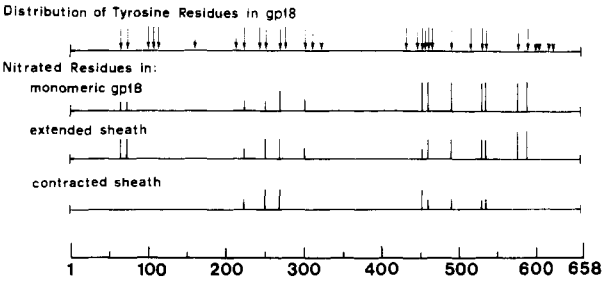

FIGURE 4: Distribution of 31 tyrosine residues and nitrated residues in gp18. Vertical arrows (including arrowheads only) above the uppermost horizontal line represent 31 tyrosine residues present in gp18. Five arrowheads without tails are for tyrosine residues whose nitration was not determined in the present study. Vertical bars, whose lengths are proportional to the number of plus signs in Table I, are for nitrated tyrosines.

Furthermore, 4 tyrosine residues in peptide K-30 were not examined due to the difficulty in quantitating the recovery of this peptide; it is 63 residues long and eluted later than K-4, which is the last peak shown in Figure 2. Nitration of a total of five tyrosines, therefore, remained undetermined. Some of them are likely to be nitrated, considering the number of total nitrated tyrosine residues (approximately 12) shown in Figure 2 and the yield of nitrated tyrosines after hydrolysis under conditions described under Materials and Methods (approximately 70% on average among major nitrated peptides). All other lysyl endopeptidase fragments that contain tyrosine residues, namely, K-5, K-7, K-13, K-15, K-17, K-21, and K-23, were not modified.

Nitration of Tyr Residues of Gp18 in the Extended Tail Sheath. After nitration of isolated tails in the presence of 5 mM $MgSO_4$, tail sheath was dissociated by 2 M urea and separated from tube–baseplates by differential ultracentrifugation. $MgSO_4$ (5 mM) was added during nitration to prevent tail sheaths from dissociation, and the intactness of the tail sheath after nitration was confirmed by electron microscopy. The resultant nitrated gp18 was analyzed with the same method as described for monomeric gp18 (Figure 2c). Although the nitration reaction proceeded slower than in the case of monomeric gp18 except for peptide K-4 (Figure 3), the nitrated residues were the same as in monomeric gp18 (Figure 4). This appears to indicate that the extended sheath structure has a sizable space between sheath protomers and between sheath and tube proteins so that the reagent, TNM, can freely

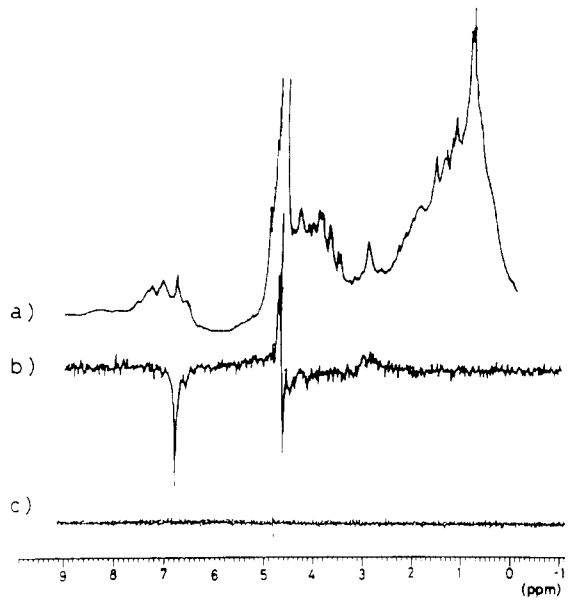

FIGURE 5: ^{1}H NMR of gp18. (a) Dark spectrum. (b) Difference photo-CIDNP spectrum. (c) Photo-CIDNP spectrum of nitrated gp18.

penetrate. Nitration of Tyr270 in peptide K-19 proceeded at almost the same rate as that for monomeric gp18, whereas Tyr63 and/or Tyr73 in peptide K-4 were/was nitrated even faster, which may reflect some conformational change of gp18 upon association.

Nitration of Tyr Residues of Gp18 in the Contracted Tail Sheath. Contracted sheaths were isolated, nitrated, and analyzed as described under Materials and Methods. Contracted sheath was more resistant to nitration than extended sheath and only eight tyrosine residues, Tyr225, -254, -270, -455, -460, -493, -532, and -535, were nitrated with reduced degrees (Figures 2d, 3, and 4). This indicated that the contracted sheath is a closely packed structure where contact areas between protomer molecules are large. This is in accord with previous results that the contracted sheath is very stable even in the presence of 6 M Gdn·HCl at room temperature (To et al., 1969).

Among eight tyrosine residues which are modifiable in the contracted sheath, Tyr270 and Tyr455 are well modified independent of the state of assembly (Table I) and considered to be exposed to the solvent regardless of the association state. Tyr270 is located in the trypsin-resistant domain (Ala82–Lys316) (Arisaka et al., 1990).

Photo-CIDNP of Monomeric Gp18. Photo-CIDNP was measured for monomeric gp18 to detect exposed aromatic side chains on the molecular surface. Figure 5 shows the normal dark spectrum (a) and the photo-CIDNP difference spectrum (b). Two peaks due to tyrosine residues were observed at 6.6 and 6.8 ppm. At least two highly exposed residues are present. These peaks disappeared when gp18 was nitrated (b). Because of the large number of nitrated tyrosine residues (13 residues), it is difficult to assign these two photo-CIDNP peaks, but it is likely that they are due to some of the tyrosine residues which are efficiently nitrated (Table I). The photo-CIDNP spectrum could not be observed for either extended or contracted sheath, because of severe line broadening of the NMR signals.

Modification of Cysteine Residues by ABD-F. There are five cysteine residues in gp18 (377, 402, 406, 477, 607); they are all in the C-terminal half of the molecule. To elucidate their state in the molecule, gp18 was modified with cysteine-specific reagent ABD-F. First, denatured gp18 was modified under the conditions reduced with tri-*n*-butylphosphine and then thoroughly digested with trypsin. The digest was applied to an HPLC column, and the eluate was monitored by fluorescence emission at 515 nm excited at 380 nm, to detect ABD-modified peptides. Four peaks were detected (Figure 6a). These peaks were isolated, rechromatographed, and analyzed for their amino acid compositions and sequences. The results have revealed that these peaks are for peptides A, Gln400–Arg410; B, Val605–Arg632; C, Gln400–Arg420; and D, Trp466–Arg479. Both peaks A and C contain Cys402 and Cys406. Apparently, the peptide linkage between Arg410 and Glu411 is somewhat resistant to trypsin, possibly due to the negative charge of Glu411. The results also indicate that the peptide bond between Arg619 and Asn620, which is preceded by Asp618, is resistant to trypsin. The Cys377-containing peptide was not observable, probably because the Arg364–Glu365 bond is resistant to trypsin and the resultant peptide Gly317–Lys390 is too long and too hydrophobic to be eluted on HPLC under the conditions used. When denatured gp18 was treated with ABD-F in the absence of tri-*n*-butylphosphine, the heights of peaks A and C decreased considerably (Figure 6b). This suggests that sulfhydryl groups of Cys402 and Cys406 form a disulfide bond.

On the other hand, to determine which sulfhydryl groups are exposed to the solvent in the native protein, native monomeric gp18 and gp18 in the extended sheath were subjected

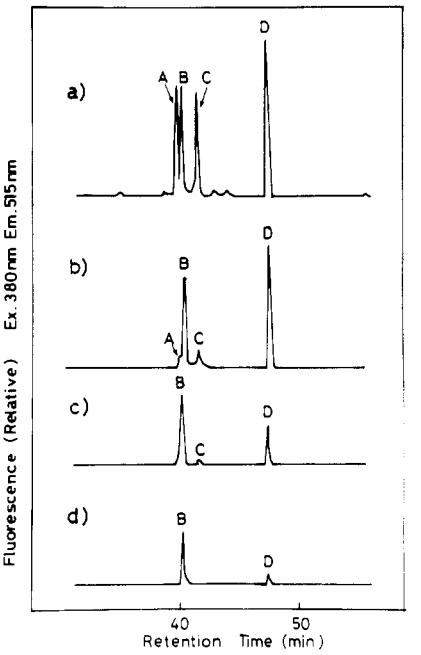

FIGURE 6: HPLC elution profiles of ABD tryptic peptides as monitored by fluorescence of ABD–cysteine residue. (a) Denatured and reduced gp18, (b) denatured and nonreduced gp18, (c) intact monomer gp18, and (d) intact extended sheath were treated with ABD-F, and the modified gp18 under each condition was digested with trypsin after heat denaturation and subjected to HPLC analysis.

Table II: Relative Peak Heights of Peptides That Contain ABD–Cysteine

peak	Cys residues present	relative peak heights: denatured and reduced	denatured and nonreduced	intact monomer	extended sheath
A	Cys402, Cys406	1.01	0.06	0.00	0.00
B	Cys607	1.00[a]	1.03	1.03	0.34
C	Cys402, Cys406	0.94	0.05	0.05	0.00
D	Cys477	1.23	1.20	0.60	0.05

[a] The corresponding peak height was taken as a standard.

to the modification. As shown in Figure 6c,d and Table II, Cys607 was modified both in the monomeric form and in the extended sheath. Cys477 was modified in the monomeric state of gp18 to some extent, but the efficiency of its modification in the extended sheath was significantly decreased. The difference of reactivity between the two cysteine residues in the extended sheath was much larger than in the monomeric form. The environment of Cys477 is such that it becomes less accessible to the modification reagent when associated into the extended sheath.

The Cys377-containing peptide was not observable in this series of experiments as mentioned above. However, our previous experiment with another fluorescent SH-specific reagent, SBD-F, has yielded a fluorescent peptide fragment containing labeled Cys377 from a tryptic digest of gp18 after treatment with this reagent under denaturing conditions in the absence of tri-*n*-butylphosphine (Nakako, Arisaka, and Ishii, unpublished results). In that experiment, a trypsin preparation which had not been affinity purified was used for digestion. Commercially available trypsin, if not further purified, always has slight contamination of chymotrypsin-like activity which cannot be totally suppressed with inhibitors such as TPCK. The fluorescent peptide yielded from the tryptic digest was Ile373–Lys390, which had been produced by the additional cleavage between Phe372 and Ile373. The presence of fluorescent label in this peptide indicates that Cys377 possesses a sulfhydryl group. Whether the sulfhydryl group of Cys377 is exposed to the solvent in the native gp18 remains to be determined.

Discussion

The present study has been designed to identify tyrosine and cysteine residues that are on the surface of the molecule. A differential chemical modification was expected to depend on the association state of the protomer gp18 molecules. There are four major conclusions from the differential chemical modification of tyrosine residues with TNM: (1) In the monomeric gp18 as well as in gp18 in the extended sheath, more tyrosine residues are nitrated in the C-terminal half of the molecule than are in the N-terminal half (Figure 4). (2) Modified tyrosine residues in the monomeric form and in the extended sheath were identical, which indicated that the extended sheath structure has a sizable space between subunit molecules in the tail. (3) Upon contraction of the tail sheath, many of the tyrosine residues in the C-terminal half became less reactive or even nonreactive and are considered to be buried or become close to the buried surface during that process. (4) There are three tyrosine residues, Tyr254, Tyr270, and Tyr455, which were nitrated independent of the association state of gp18. Two of them were in the trypsin-resistant fragment (Ala82–Lys316), which is suggested to constitute the protruding part of gp18 [Figure 7; also see Arisaka et al. (1990)]. Furthermore, a chemical modification study of cysteine residues with ABD-F has shown that Cys377, -477, and -607 have a free sulfhydryl group and that Cys402 and Cys406 are very likely to form a disulfide bridge.

Precautions have to be taken for the interpretation of the results of chemical modification. For example, nitration of one tyrosine residue possibly makes another one, which was originally buried, accessible to TNM. It is, therefore, important to assure that the chemical modification does not change the conformation of target protein molecules. In the present experiments, this was done by CD spectrum measurement in the far-UV region in the case of monomeric gp18 and by measuring the kinetics of the modification for monomeric gp18 and for extended sheath. From the absence of a significant change in the CD spectrum up to 90 min, it was concluded that at least secondary structures remained intact. Kinetic measurements have indicated that the time course of nitration for each tyrosine residue in the monomeric gp18 or in the extended sheath is more or less the same (Figure 3). Furthermore, nitration reached a plateau at around 90 min, and no further nitration occurred, which also indicated that no unfolding or drastic conformational change took place. Although we cannot completely exclude the possibility of partial distortion by nitration of some residues (see next paragraph), most of the nitration is considered to reflect the accessibility of tyrosine residues in the intact protein to TNM. Also, note that our emphasis has been to detect the difference of nitration among three states of association, namely, monomeric gp18, extended sheath, and contracted sheath.

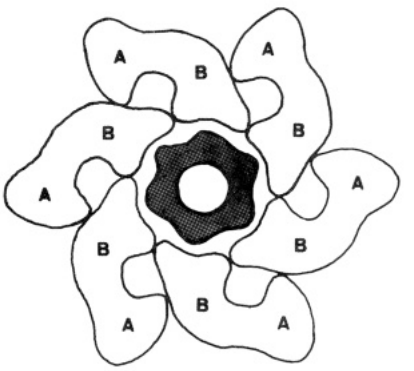

FIGURE 7: Cross section of the cocylindrical structure of a tail with extended sheath [redrawn from Plate VIa of Amos and Klug (1975)]. Experimental results are all compatible with a model in which region A corresponds to the protease-resistant, chemically less modifiable rigid domain and region B corresponds to the C-terminal half of the molecule which is chemically more modifiable and has a relatively flexible structure. Tyr270 (in region A) and Tyr455 (in region B), which were nitrated regardless of the association state of gp18, are considered to be located on the surface of the sheath facing the solvent. Flexibility in region B is possibly important for the assembly and contraction of the tail sheath.

Iodination as well as nitration is often employed in differentiating the accessibility of tyrosine residues in protein molecules. One has to be cautious about concluding which residues are on the surface of the molecule on the basis of these methods. In the case of bovine pancreatic trypsin inhibitor (BPTI), TNM nitrated specifically two tyrosine residues that are known to be exposed on the surface of the molecule as determined by X-ray crystallography. However, iodination with I_3^- occurred not only on these two tyrosine residues but also on the third one which is buried in the molecule (Sherman & Kassell, 1968; Kaptein et al., 1978). In the case of cytochrome *c*, two internal tyrosine residues (Tyr48 and Tyr67) are more reactive toward TNM than are the other two at the surface of the molecule (Tyr74 and Tyr97; Creighton, 1984). In contrast, iodination modifies primarily Tyr67 and Tyr74. We, therefore, do not conclusively argue that all the TNM-reactive tyrosine residues in gp18 are on the surface of the molecule. Instead, our emphasis is on the difference in modification which depends on the association state of the tail sheath protein: contracted sheath is the least modifiable structure, but some residues in the contracted sheath such as Tyr270 are still readily modifiable.

Tail tube was also treated with TNM, but no nitrated residues were detected (data not shown). All four tyrosines in tail tube protein, gp19, therefore, appear to be buried in the tail tube structure.

Among those cysteine residues which have a sulfhydryl group, namely, Cys377, -477, and -607, at least the groups

of Cys477 and Cys607 are modifiable in the native monomer molecule. Although the rate of modification somewhat decreased, the SH group of Cys607 is reactive even in the extended sheath. When monomeric gp18 was modified with ABD-F, it appeared to lose polymerization ability into either extended sheath or polysheath. The result may be utilized to grow a single crystal of gp18 for X-ray diffraction analysis.

It is very likely that SH groups of Cys402 and Cys406 form a disulfide bond, although we have not been successful in isolating the cystine-containing peptide. It may be noted in Figure 6 that peaks A and C which contain Cys402 and Cys406 are not totally absent. It appears that some fraction, approximately 15%, of the disulfide between these cysteines is reduced in native gp18. It is generally believed that the redox potential of the cytosol in bacteria is such that disulfide bonds are not spontaneously formed in the cell. The disulfide bond between Cys402 and Cys406 is probably formed outside the cell after lysis. This is in contrast with the case of eucaryotes where disulfide isomerase in the microsome may efficiently regulate the disulfide formation so that complete disulfide formation takes place, although details of the cellular function of the enzyme is not known (Creighton, 1984).

Chemical modification is one of the approaches we have used to elucidate the structure–function relationship of the contractile tail sheath protein of bacteriophage T4. In the accompanying paper, we report the results of limited proteolysis, immunoblotting, and immunoelectron microscopy.

Acknowledgments

We thank Professor Edward Goldberg for invaluable comments on the manuscript. We also thank Dr. K. Imai for kindly providing us with SBD-F and ABD-F and Drs. F. Hayashi and B.-J. Lee for NMR measurements.

Registry No. Tyr, 60-18-4; Cys, 52-90-4.

References

Amos, L. A., & Klug, A. (1975) *J. Mol. Biol. 99*, 51–73.

Arisaka, F., Nakako, T., Takahashi, H., & Ishii, S. (1988) *J. Virol. 62*, 1186–1193.

Arisaka, F., Takeda, S., Funane, K., Nishijima, N., & Ishii, S. (1990) *Biochemistry* (following paper in this issue).

Black, L. W., & Showe, M. K. (1983) in *Bacteriophage T4* (Matthews, C. K., Kutter, E. M., Mosig, G., & Berget, P. B., Eds.) pp 219–245, American Society for Microbiology, Washington, DC.

Brenner, S., Streisinger, G., Horne, R. W., Champe, S. P., Barnett, L., Benzer, S., & Rees, M. W. (1959) *J. Mol. Biol. 1*, 281–292.

Creighton, T. E. (1984) in *PROTEINS, Structure and Molecular Properties*, pp 272–276, Freeman, New York.

Crowther, R. A., Lenk, E. V., Kikuchi, Y., & King, J. (1977) *J. Mol. Biol. 116*, 489–523.

Dickson, R. C. (1974) *Virology 59*, 123–138.

Favre, R., Boy de la Tour, E., Segre, N., & Kellenberger, E. (1965) *J. Ultrastruct. Res. 13*, 318–342.

Kaptein, R., Dijkstra, K., & Nicolay, K. (1978) *Nature 274*, 293–294.

Kellenberger, E. (1968) *Virology 34*, 549–561.

Kellenberger, E., & Boy de la Tour, E. (1964) *J. Ultrastruct. Res. 11*, 545–563.

King, J., & Mykolajewycz, N. (1973) *J. Mol. Biol. 75*, 339–358.

Kumazaki, T., Nakako, T., Arisaka, F., & Ishii, S. (1986) *Proteins 1*, 100–107.

Moody, M. F. (1973) *J. Mol. Biol. 60*, 613–635.

Ruegg, U. T., & Rudinger, J. (1977) *Methods Enzymol. 77*, 111–116.

Sarkar, N., Sarkar, S., & Kozloff, L. M. (1964) *Biochemistry 3*, 517–522.

Sherman, M. P., & Kassell, B. (1968) *Biochemistry 7*, 3643–3641.

Simon, L. D., & Anderson, T. F. (1967) *Virology 32*, 298–305.

To, C. M., Kellenberger, E., & Eisenstark, A. (1969) *J. Mol. Biol. 46*, 493–511.

Toyo'oka, T., & Imai, K. (1984) *Anal. Chem. 56*, 2461–2464.

Tschopp, J., Arisaka, F., van Driel, R., & Engel, J. (1979) *J. Mol. Biol. 128*, 281–286.

Yanagida, M. (1972) *J. Mol. Biol. 65*, 501–517.